A pH-sensitive stearoyl-PEG-poly(methacryloyl sulfadimethoxine)-decorated liposome system for protein delivery: An application for bladder cancer treatment

Marian Vila-Caballer, Gaia Codolo, Fabio Munari, Alessio Malfanti, Matteo Fassan, Massimo Rugge, Anna Balasso, Marina de Bernard, Stefano Salmaso

PII: S0168-3659(16)30458-8
DOI: doi: 10.1016/j.jconrel.2016.07.024
Reference: COREL 8381

To appear in: *Journal of Controlled Release*

Received date: 9 March 2016
Revised date: 5 July 2016
Accepted date: 15 July 2016

Please cite this article as: Marian Vila-Caballer, Gaia Codolo, Fabio Munari, Alessio Malfanti, Matteo Fassan, Massimo Rugge, Anna Balasso, Marina de Bernard, Stefano Salmaso, A pH-sensitive stearoyl-PEG-poly(methacryloyl sulfadimethoxine)-decorated liposome system for protein delivery: An application for bladder cancer treatment, *Journal of Controlled Release* (2016), doi: 10.1016/j.jconrel.2016.07.024

A pH-sensitive stearoyl-PEG-poly(methacryloyl sulfadimethoxine)-decorated liposome system for protein delivery: an application for bladder cancer treatment

Marian Vila-Caballer[a,1], Gaia Codolo[a], Fabio Munari[b], Alessio Malfanti[c], Matteo Fassan[d], Massimo Rugge[d], Anna Balasso[c], Marina de Bernard[a,*], Stefano Salmaso[c,*]

[a]Department of Biology, University of Padova, Via U. Bassi, 58/B, 35121 Padova, Italy
[b]Department of Biomedical Sciences, University of Padova, Via Ugo Bassi 58/B, 35121 Padova, Italy.
[c]Department of Pharmaceutical and Pharmacological Sciences, University of Padova, Via Marzolo, 5, 35131 Padova, Italy.
[d]Surgical Pathology and Cytopathology Unit, Department of Medicine, University of Padova, Via Aristide Gabelli, 61, 35121 Padova, Italy.
[1]Present address: Department of Biomedical Sciences, University CEU Cardenal Herrera, Avda. Seminario s/n., 46113 Moncada, Valencia, Spain.
*Corresponding authors: stefano.salmaso@unipd.it, marina.debernard@unipd.it

Key words: pH-responsive liposomes, tumour targeting, protein delivery, bladder cancer treatment

Abstract

Stealth pH-responsive liposomes for the delivery of therapeutic proteins to the bladder epithelium were prepared using methoxy-poly(ethylene glycol)$_{5kDa}$-1,2-distearoyl-sn-glycero-3-phosphoethanolamine (mPEG$_{5kDa}$-DSPE) and stearoyl-poly(ethylene glycol)-poly(methacryloyl sulfadimethoxine) copolymer (stearoyl-PEG-polySDM), which possesses an apparent pKa of 7.2. Liposomes of 0.2:0.6:100, 0.5:1.5:100 and 1:3:100 mPEG$_{5kDa}$-DSPE/stearoyl-PEG-polySDM/(soybean phosphatidylcholine + cholesterol) molar ratios were loaded with bovine serum albumin (BSA) as a protein model. The loading capacity was 1.3% w/w BSA/lipid. At pH 7.4, all liposome formulations displayed a negative zeta-potential and were stable for several days at pH 7.4. By pH decrease or addition to mouse urine, the zeta potential strongly decreased, and the liposomes underwent a rapid size increase and aggregation. Photon correlation spectroscopy (PCS) and transmission electron microscopy (TEM) analyses showed that the extent of the aggregation depended on the stearoyl-PEG-polySDM/lipid molar ratio. Cytofluorimetric analysis and confocal microscopy showed that at pH 6.5, the incubation of MB49 mouse bladder cancer cells and macrophages with fluorescein isothiocyanate-labelled-BSA (FITC-BSA) loaded and N-(Lissamine Rhodamine B sulfonyl)-1, 2-dihexadecanoyl-sn-glycero-3-phosphoethanolamine triethylammonium salt (rhodamine-DHPE) labelled 1:3:100 mPEG$_{5kDa}$-DSPE/stearoyl-PEG-polySDM/lipid molar ratio liposomes resulted in a time-dependent liposome association with the cells. At pH 7.4, the association of BSA-loaded liposomes with the MB49 cells and macrophages was remarkably lower than at pH 6.5. Confocal images of bladder sections revealed that 2 h after the instillation, liposomes at pH 7.4 and control non-responsive liposomes at pH 7.4 or 6.5 did not associate nor delivered FITC-BSA to the bladder epithelium. On the contrary, the pH-responsive liposome formulation set at pH 6.5 and soon administered to mice by bladder instillation showed that, 2 h after administration, the pH-responsive liposomes efficiently delivered the loaded FITC-BSA to the bladder epithelium.

1. Introduction

Bladder cancer is the fifth most common malignancy in the world with non-muscle-invasive bladder cancer comprising 70% of newly diagnosed bladder cancers [1]. The gold standard treatment of this neoplasia in the early stages is a trans-urethral resection followed by intravesical immunotherapy with Bacillus Calmette-Guérin (BCG). However, a large fraction of patients does not respond to the treatment, and severe side effects are associated to this therapy [2]. Therefore, alternative or complementary strategies for the management of non-muscle-invasive bladder cancer are needed [3]. Among the biological therapies, Interferon-alpha (IFN-α) has been successfully applied in initial early-phase clinical studies, especially in combination with BCG immunotherapy [4]. Atezolizumab is a humanized antibody recently approved by FDA for bladder cancer treatment [5] while the 38 kDa immunomodulator PstS1 obtained from the *Mycobacterium tuberculosis* is currently under clinical trials [6]. In the recent past, the neutrophil-activating protein (HP-NAP) produced by the bacterium *Helicobacter pylori* has been shown to inhibit bladder cancer growth in a mouse model [7]. However, the low residence time of a therapeutic biologic in the bladder, which mainly does not last beyond the first bladder emptying, requires large doses and frequent instillations to achieve a therapeutic effect.

Several efforts have been devoted to generate drug delivery systems to target bladder cancer, including gold nanoparticles [8], mucoadhesive cationic particles [9-12], gelatine-based nanosystems [13,14], and albumin-based nanoparticles [15]. Liposomes have never been explored for the delivery of proteins and peptides for treatment of bladder cancer [16]. On the other hand, they have been successfully used to deliver peptides, synthetic lipopeptides and proteins for a variety of applications including: vaccination [17], cell-targeting and intracellular delivery [18,19], cell activation [20], imaging [21,22], theranostic applications [23], treatment of cerebrovascular diseases [24], ocular inflammation [23], pulmonary artery hypertension [25], restenosis [26], lysosomal storage diseases [27,28], and cancer [29]. Notably, liposomes have been considered as vehicle for local administration of BCG [30,31] and anticancer drugs for the treatment of bladder cancer [32,33] as well as for the treatment of a variety of urinary tract disorders such as interstitial cystitis/painful bladder syndrome [34], haemorrhagic cystitis [35] and

refractory overactive bladder [36]. Moreover, liposomes do not alter the urothelium in comparison to other delivery systems, such as micelles [37].

In a previous study, we reported the preparation of biocompatible pH-responsive liposomes that, upon exposure to acidic pH, underwent aggregation due to the loss of surface charge and associated with cells [38]. This behaviour provides for the liposomal selective response to acidic environments, such as in solid tumours [39] or in the bladder cavity [40]. In this study, we investigated the biophysical properties of a pH sensitive liposome formulation and explored it as delivery vehicle of proteins to macrophages, cancer cells and epithelium of the bladder with the aim to put forward an alternative to the existing standard of care for bladder cancer treatment (namely BCG) [41] that may cause harsh local inflammation and bacterial infection [42]. The responsive system we discuss here, in virtue of its epithelium adhesive properties, may enhance the outcome of therapeutic proteins when locally administered by increasing the exposure time of the bladder epithelium and the local bioavailability.

2. Materials and methods

Cholesterol, 4.67 kDa polyoxyethylene stearyl ether (Brij-700®), foetal bovine serum (FBS) and Float-A-Lyzer® G2 300 kD molecular weight cut-off (MWCO) dialysis devices were provided by Sigma-Aldrich (St. Louis, MO, USA). Soybean phosphatidylcholine (Epikuron 200, SPC) was furnished by Cargill (Minneapolis, MN, USA). Methoxy-poly(ethylene glycol)$_{5kDa}$-1,2-distearoyl-sn-glycero-3-phosphoethanolamine (ammonium salt) (mPEG$_{5kDa}$-DSPE) resulting from the condensation of 5 kDa methoxy-poly(ethylene glycol)-COOH and 1,2-distearoyl-sn-glycero-3-phosphoethanolamine was purchased from JenKem Technology USA, Inc. (Allen, TX, USA), and N-(Lissamine Rhodamine B sulfonyl)-1, 2-dihexadecanoyl-sn-glycero-3-phosphoethanolamine, triethylammonium salt (rhodamine-DHPE) was obtained from VWR International PBI (Radnor, PA, USA). Alexa Fluor 647-Cholera Toxin Subunit B was purchased from Molecular Probes (Waltham, MA, USA). Stearoyl-PEG-polySDM and fluorescein isothiocyanate labelled bovine serum albumin (FITC-BSA) were synthetized as previously described [38,43]. The chemical structures of lipids and of lipid conjugates are reported in Scheme S1.

Sterile 0.2 µm PTFE Millex® syringe filters and 0.2 µm PES Corning® syringe filters were purchased from Sigma-Aldrich (St. Louis, MO, USA). All buffer salts, other reagents and solvents were purchased from VWR International PBI (Radnor, PA, USA), Sigma-Aldrich (St. Louis, MO, USA) and J.T. Baker (Phillipsburg, NJ, USA) and were of analytical or HPLC grade unless stated otherwise. All the reagents used for cell studies (unless indicated) were purchased from Sigma-Aldrich (St. Louis, MO, USA).

2.1. Liposome preparation and protein loading studies

BSA-loaded liposomes were prepared using a 2:1 soybean phosphatidylcholine/cholesterol molar ratio lipid mixture according to the thin layer rehydration technique [44]. Formulations were prepared using 5 or 10 mg/mL lipid concentrations and 0.2, 0.5, 1 or 2 mg/mL BSA according to the procedure previously described [38]. Briefly, 5 or 10 mg of lipids were dissolved in 3 mL of anhydrous chloroform. The lipid solution was filter-sterilized using 0.2 µm PTFE Millex® syringe filters. The organic solvent was removed under reduced pressure using a rotary evaporator and stored overnight under vacuum. A 20 mg/mL BSA stock solution in PBS at pH 7.4 was filter-sterilized using 0.2 µm PES Corning® syringe filters. The BSA content in the solution was assessed by UV-Vis spectroscopy and UPLC chromatography. The lipid film was rehydrated with 100 µL of a 2, 5, 10 or 20 mg/mL BSA solution in PBS at pH 7.4 and processed with 10 freeze-thawing cycles. The samples were then diluted to 1 mL with the same buffer and finally extruded 11 times through a polycarbonate membrane with a 200-nm cut-off (Nuclepore, Pleasanton, CA, USA). The non-loaded BSA was removed by dialysis according to a validated protocol [45]; 1 mL of liposomes was dialyzed using a 300-kDa Float-A-Lyser® G2 system against 1 L of PBS at pH 7.4. The liposome loading efficiency and capacity were assessed after dialysis by reverse phase ultra-performance liquid chromatography (UPLC, Agilent, Santa Clara, CA, USA) equipped with a Phenomenex ZORBAX RRHD column (150 x 2.1 mm) loaded with stationary phase Eclipse Plus C18 (Dikma, Lake Forest, CA, USA) and isocratically eluted at 0.2 mL/min with a 90:10 v/v mixture of H_2O/acetonitrile both supplemented with 1% v/v of formic acid. The UV detector was set at 220 nm. The BSA concentration (y) was determined from the peak area (x) using a standard curve

obtained with BSA solutions of known concentrations [y (μg BSA/mL) = 0.0178 x (peak area) – 5.3054; R^2 = 0.99979]. The encapsulation efficiency was calculated as the amount of loaded BSA after dialysis and expressed as the percentage of the BSA fed to hydrate the liposomes. The liposome loading capacity was expressed as the amount of encapsulated BSA (after dialysis) per mg of lipid.

PEGylated liposomes were prepared using 10 mg of lipids and 1 mg BSA according to the procedure reported above to obtain a final volume of 1 mL. A 8 mg/mL $mPEG_{5kDa}$-DSPE solution in PBS, pH 7.4, was filter-sterilized using 0.2 μm PES Corning® syringe filters and was added to the lipid vesicles to obtain 0.2:100, 0.5:100, and 1:100 $mPEG_{5kDa}$-DSPE/lipids mol%. Liposomes were dialyzed as reported above to remove the non-encapsulated BSA, and the liposome loading efficiency and capacity were evaluated.

A 25 mg/mL stock solution of stearoyl-PEG-polySDM in PBS, pH 7.4 was filter-sterilized using 0.2 μm PES Corning® syringe filters. Stealth pH-responsive liposomes (pH-RL) were prepared by adding proper volumes of the stearoyl-PEG-polySDM stock solution to the $mPEG_{5kDa}$-DSPE decorated liposomes described above to obtain: 0.2:0.6:100, 0.5:1.5:100, or 1:3:100 $mPEG_{5kDa}$-DSPE/stearoyl-PEG-polySDM/lipids mol% (0.2:0.6-pH-RL, 0.5:1.5-pH-RL and 1:3-pH-RL, respectively). The formulations were incubated at 37 °C for 1 h before proceeding with the experiments.

Non-pH-responsive formulations used as control liposomes (0.2:0.6-CL, 0.5:1.5-CL and 1:3-CL) were prepared as reported above for pH-RL by replacing the stearoyl-PEG-polySDM with equimolar amounts of Brij-700®.

Fluorescently double-labelled liposomes 1:3-pH-RL and 1:3-CL were prepared for cell treatments and *in vivo* tests by adding 0.1 mol% of rhodamine-DHPE (Biotium, Hayward, CA, USA) to the chloroform lipid mixture (10 mg/mL of lipids in the final liposome formulation). One mg/mL FITC-BSA in PBS, pH 7.4, was used to rehydrate the lipid films. Fluorescent liposomes were prepared as above. Rhodamine-DHPE-labelled liposomes containing non-labelled BSA and unlabelled liposomes loaded with FITC-BSA were used as controls.

All procedures were performed under sterile conditions.

2.2. Liposome characterization: size and zeta potential analysis and TEM imaging

Size, polydispersity index (PDI) and zeta potential were measured by Photon correlation spectroscopy (PCS) using a Zetasizer NanoZS (Malvern Instruments Ltd., UK). Results of size analysis were expressed as Z-average. Liposome samples (0.5 mg/mL final lipid concentration) in PBS, pH 7.4, were analysed at days 0, 2, 5, 7, 9, 12, 16, 19 and 48 at 25 °C and 37 °C. Liposome samples (0.5 mg/mL final lipid concentration) were prepared by 20-fold dilution of the stock liposome suspension (10 mg/mL lipid concentration in PBS at pH 7.4) with PBS, pH 6.5 and 7.4, and were analysed at 0, 0.5, 1, 2, 4, 6 and 24 h at 25 °C and 37 °C. Time "zero" corresponded to 1 min after pH setting.

A size analysis of 1:3-CL and 1:3-pH-RL (0.5 mg/mL final lipid concentration), prepared by 20-fold dilution of the stock liposome suspension as reported above, was also carried out at different pHs ranging from 6.5 to 7.4 and in mouse urine.

The zeta potential was determined applying a voltage of 40 V.

A transmission electron microscopy (TEM) analysis was performed using a FEI Tecnai G2 microscope (Hillsboro, OR, USA). Liposomes (0.5 mg/mL final lipid concentration) in PBS, pH 7.4 and 6.5, were laid down on a carbon-coated copper grid at time 1 h. The excess volume was removed using filter paper, and the samples were negatively stained with 1% uranyl acetate in distilled water and analysed.

2.3. Evaluation of protein release

Two mL of each of the liposome formulations was transferred into a Float-A-Lyzer® G2 300 kDa MWCO dialysis device and placed in 1 L of PBS, pH 7.4 or 6.5 at 25 °C and 37 °C. At 1, 2, 4, 6, 24, 48, 72, 96, 120, 144, 168, 192, 216, 240 h, aliquots of the liposome samples (100 µL) were withdrawn, and the BSA content was quantified by reverse phase UPLC analysis as described above. The amount of released BSA was calculated by subtracting the amount of BSA in the donor compartment (non-released BSA) from the initial amount in the dialysis device by referring to the standard titration curve reported above.

2.4. Evaluation of liposome association to the cells

MB49 mouse bladder cancer cells (kindly provided by Prof. Michael O'Donnell, University of Iowa, Iowa City, IA-USA) and THP-1 human monocytes (purchased from ATCC®) were grown in RPMI-1640 medium supplemented with 10% FBS. The MB49 and THP-1 cells were seeded on 24-well plates (2×10^5 per well). The THP-1 cells were differentiated to macrophages by adding 100 ng/mL phorbol 12-myristate 13-acetate (PMA) to the medium and left to differentiate for 48 h [46]. The medium was removed, and the cells were washed twice. $NaHCO_3$-free DMEM-based medium supplemented with 10 mM Na_2HPO_4 and 4 mM HEPES was used to wash MB49 cells. PBS supplemented with 2 mg/mL glucose and 0.3 mg/mL glutamine was used to wash THP-1-derived macrophages (TDM). The media were optimized to ensure cell viability and constant pH during the experiments. Next, the cells were incubated with 0.5 mg/mL of FITC-BSA-loaded rhodamine-DHPE labelled 1:3-CL or 1:3-pH-RL in minimum medium, pH 7.4 or 6.5, for 0.5, 1, 2, 4 and 6 h.

BSA-loaded unlabelled liposomes, rhodamine-DHPE-labelled liposomes and FITC-BSA-loaded unlabelled liposomes were used to define the fluorescence background and fluorescence leakage.

Cytofluorimetric analyses. Cells were washed twice with PBS, collected by scraping, recovered by centrifugation and fixed with 3.7% (w/v) paraformaldehyde in PBS. The cells were then analysed using a BD FACSCanto instrument equipped with BD FACSDiva software (Becton Dickinson, Franklin Lakes, NJ, USA) and gated using forward *vs*. side scatter to exclude debris and dead cells. The double FITC- and rhodamine-stained cell population was analysed.

Confocal microscopy. Cells were seeded on 24-chamber glass slides (Sigma–Aldrich, St. Louis, MO, USA). After the incubation with liposomes, the cells were washed twice with PBS and then fixed with 3.7% (w/v) paraformaldehyde in PBS. The cell membranes were labelled with 10 μg/mL of Alexa Fluor 647-Cholera Toxin Subunit B. The nuclei were stained with DAPI. A confocal analysis was performed using a Leica TCS SP5 II confocal laser-scanning microscope equipped with Leica HCX PL APO lambda blue 40x/1.25 and 63x/1.4 OIL UV lenses and Leica Application Suite AF software (Leica Microsystems, Mannheim, Germany). Lasers at 405, 488, 560 and 633 nm were used to

detect the fluorescence of DAPI, FITC, rhodamine and Alexa Fluor 647, respectively and emission was recovered at a bandwidth centred at 461, 525, 580 and 660 nm, respectively. The localization of liposomes, BSA and cell membrane was derived by a line-scan analysis of single fluorophores (rhodamine, FITC, and Alexa Fluor 647) along a cellular section. The quantification of the co-localization between the fluorescent signal from rhodamine and that from FITC, per single cell, was also performed. At least 10 fields were analysed for each condition. Image analyses were performed using ImageJ 1.47v (National Institutes of Health software package).

2.5. *In vivo* studies

The in vivo studies were carried out using three-month-old female C57BL/6J mice. Mouse urine samples were obtained one week before the mice were treated with the liposome formulations. To this aim, mice were maintained in a metabolic cage overnight (12 h) with *ad libitum* access to food and water, and the urine was collected.

Before the liposome administration, the mice were anesthetized by intra-peritoneal injection of a Zoletil (Virbac, Carros cedex, France) and Xylazine (VetTech, Middleburg, VA, USA) mix (40 mg/Kg and 5 mg/Kg, respectively) and catheterized via the urethra with a 24-gauge plastic intravenous cannula. Bladders were washed with PBS at pH 7.4 or 6.5 as appropriate and then instilled with 150 µL of the liposome formulation (10 mg/mL final lipid concentration) at pH 6.5 and 7.4, 1 min after the pH was set, when required, with 1 N HCl addition. The mice were divided in 4 groups (N=3 for each group) and the bladders were instilled with FITC-BSA-loaded rhodamine-DHPE-labelled liposomes: 1:3-pH-RL at pH 7.4; 1:3-pH-RL at pH 6.5; 1:3-CL at pH 7.4; 1:3-CL at pH 6.5. The formulations were instilled through the cannula and maintained within the bladder for 2 h to prevent premature bladder evacuation. The bladder contents were carefully removed, and the cavities were washed twice with 150 µL PBS at pH 7.4 or 6.5. The mice were euthanized by cervical dislocation, and the bladders were excised and embedded in Optimal Cutting Temperature Tissue Freezing Medium. The specimens were cut with a cryostat Leica CM1850 (Leica Microsystems, Mannheim, Germany) to obtain 4 µm thick histological sections. The slices were mounted and analysed by confocal microscopy as described above.

The mice were handled by specialized personnel under the control of inspectors of the Veterinary Service of the Local Sanitary Service. All *in vivo* procedures were carried out according the EU and NIH directives and approved by the Italian Ministry of Health (authorization number 54/2014).

2.6. Statistical analysis

Data were processed using either a two-tailed unpaired Student's *t* test or analysis of variance (ANOVA), followed by either Bonferroni or, when necessary, Games–Howell post hoc test (SPSS statistical software; IBM, Armonk, NY). Levene's test was used to determine homogeneity of variances. Values of $p \leq 0.05$ were considered statistically significant.

3. Results

3.1. Evaluation of liposome loading capacity

The preliminary studies were aimed at selecting suitable conditions for the preparation of protein-loaded liposome formulations. BSA was used as protein model, and the effect of the lipid/protein ratio on the protein loading efficiency and capacity was investigated. Data reported in Figure 1 show that the loading efficiency decreased and the loading capacity increased as the protein concentration in the rehydrating buffer increased, as reported in the literature [47]. The maximal loading efficiency (13 µg BSA/mg lipids) was obtained with a 10 mg/mL lipid concentration and a 0.2 mg/mL BSA concentration in the rehydrating buffer (Figure 1A), while the maximal loading capacity was obtained with 2 mg/mL BSA (Figure 1B).

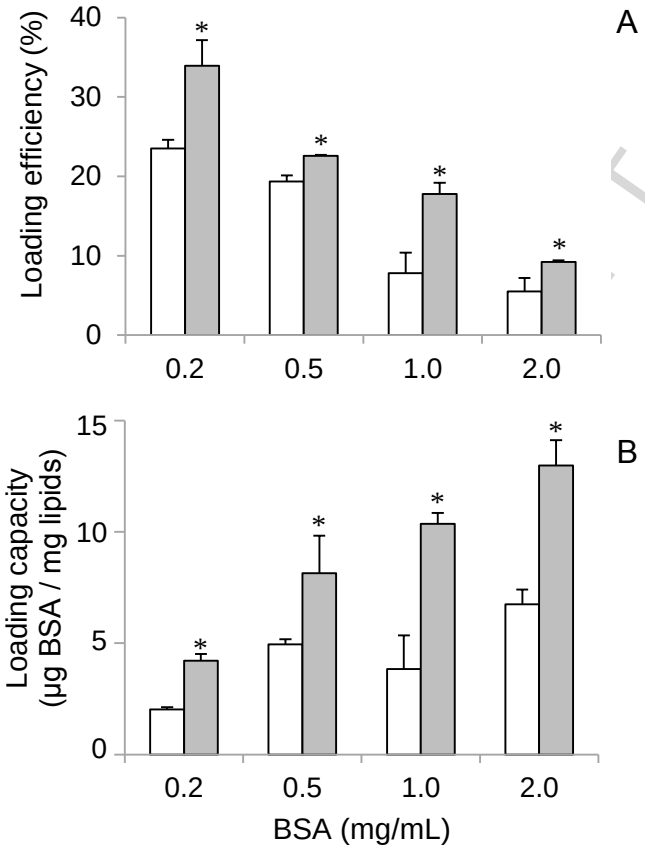

Figure 1. Effect of lipid and BSA concentration in the rehydrating buffer on encapsulation efficiency (A) and capacity (B) of the protein in liposomes. Liposomes were generated at lipid concentrations of 5 (□) and 10 (■) mg/mL. * $p < 0.05$ refers to the formulations obtained with 10 mg/mL lipids *vs* 5 mg/mL lipids at each BSA concentration.

According to these results and to the evidence that a higher protein concentration in the rehydrating buffer required a longer dialysis to remove the non-loaded BSA, the liposomal formulation obtained by rehydrating lipids at 10 mg/mL with a buffer containing 1 mg/mL BSA was selected.

The BSA quantification after dialysis (Figure S2 A, B, C and D) showed that the post-insertion of $mPEG_{5kDa}$-DSPE and stearoyl-PEG-polySDM to the liposomal formulation did not affect the protein payload.

3.2. Liposome size analysis and effect of pH

pH-responsive liposomes with the following composition were generated and analysed: 0.2:0.6:100, 0.5:1.5:100, and 1:3:100 $mPEG_{5kDa}$-DSPE/stearoyl-PEG-polySDM/lipids mol% (0.2:0.6-pH-RL, 0.5:1.5-pH-RL and 1:3-pH-RL, respectively). Control liposomes had the following composition: 0.2:0.6:100, 0.5:1.5:100, or 1:3:100 $mPEG_{5kDa}$-DSPE/Brij-700®®/lipids mol% (0.2:0.6-CL, 0.5:1.5-CL and 1:3-CL, respectively).

Size analyses of BSA-loaded pH-RL were performed by dynamic light scattering (DLS) at pH 7.4 and at pH 6.5 to mimic the human urine. Figure 2A, C and E, and supplementary Figure S3A, C and E show that at pH 7.4 the preparation process, including freeze-thaw, extrusion and incubation at 37 °C [44], yielded 0.2:0.6-pH-RL, 0.5:1.5-pH-RL and 1:3-pH-RL liposomes with size of 287 ± 10.7 nm (PDI 0.5 ± 0.07), 235 ± 8.4 nm (PDI 0.2 ± 0.04), and 167 ± 1.6 nm (PDI 0.2 ± 0.03), respectively. After 30 min exposure to acidic pH, both the mean size and PDI of all formulations considerably increased. Liposomes were considered to be in the aggregated state when size exceeded 1000 nm or PDI was 1. This occurred for the 0.5:1.5 and 1:3 pH-RL after 30 min incubation at pH 6.5. At pH 6.5, the 0.2:0.6-pH-RL and 0.5:1.5-pH-RL liposomes reached the maximum size in 1-2 h incubation, while the 1:3-pH-RL formulation showed a progressive size increase up to several μm in 6 h. Notably, under these conditions, the size increase profile of the liposomes depended on the $mPEG_{5kDa}$-DSPE/stearoyl-PEG-polySDM/lipids molar ratio. For example, after 2 h incubation at pH 6.5 the size of 0.2:0.6-pH-RL, 0.5:1-pH-RL and 1:3-pH-RL liposomes was 755 ± 289 nm (PDI 0.92 ± 0.07), 2,069 ± 436 nm (PDI 0.86±0.28) and 3,602 ± 844 nm (PDI 1), respectively. The size increase paralleled a significant PDI increase, which indicates that under these conditions the lipid vesicles underwent macroscopic and inhomogeneous structural alterations.

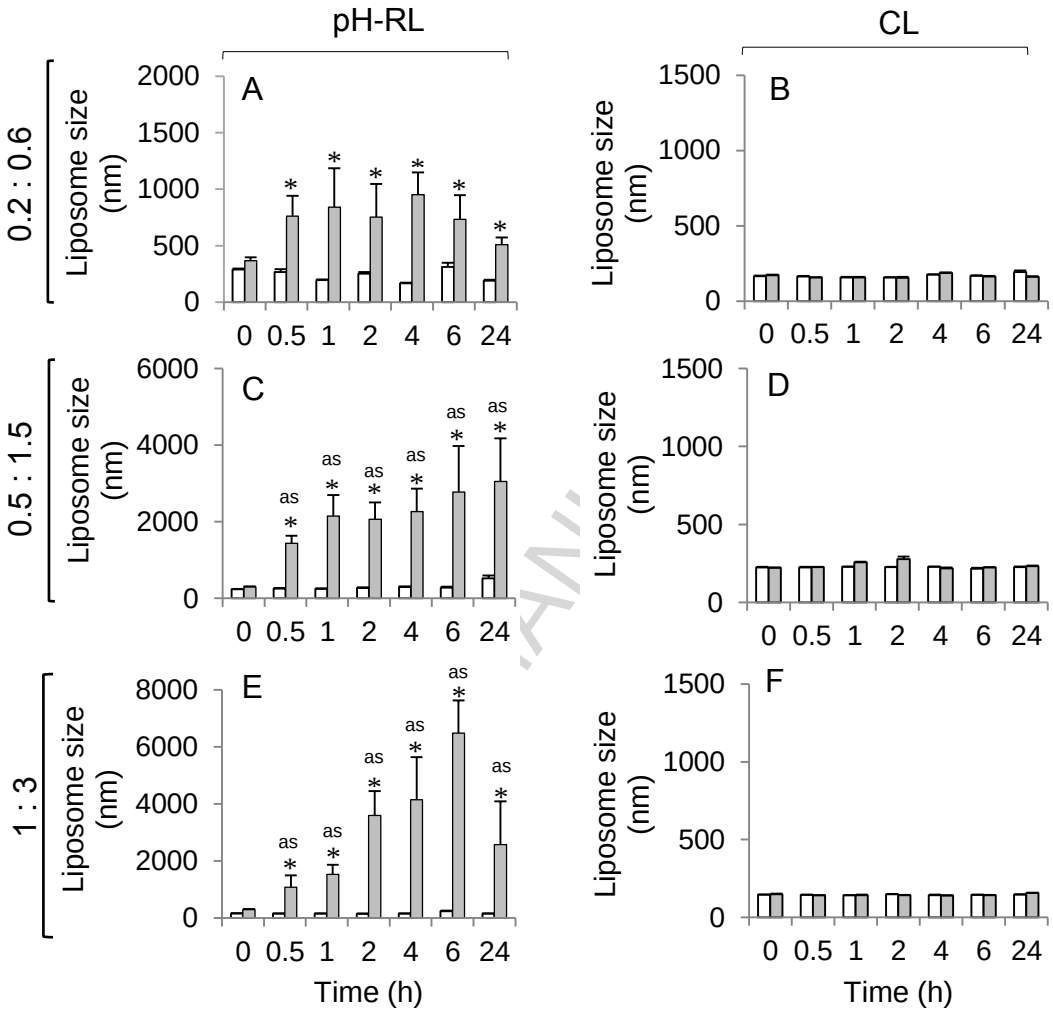

Figure 2. Time course of the size profile of 0.2:0.6-pH-RL (A), 0.2:0.6-CL (B), 0.5:1.5-pH-RL (C), 0.5:1.5-CL (D), 1:3-pH-RL (E), and 1:3-CL (F) in PBS at pH 7.4 (□) and 6.5 (■) at 25 °C. "as": aggregated state. * $p < 0.05$ refers to formulations incubated at pH 6.5 *vs* pH 7.4 at each time point.

Non-pH-responsive control liposomes (CL) obtained using Brij-700® instead of the pH-responsive stearoyl-PEG-polySDM copolymer did not undergo size and PDI alterations upon exposure to acidic pH. Figure 2B, D and F, and supplementary Figure S2B, D and F show that the sizes ranged from 146 ± 1.2 nm to 223 ± 3.7 nm and PDIs ranged from 0.12 ± 0.04 to 0.35 ± 0.03.

The time course size profiles of the 1:3-pH-RL formulation in the pH range of 7.4-6.5 depicted in Figure 3A show that these liposomes underwent an immediate size increase

as the pH was lowered below 6.7. The pH conditions close to neutrality (7.0 and 7.2) required at least 6 h to induce liposome aggregation (Figure 3A). Notably, the figure shows that these liposomes also underwent a size increase in the mouse urine with a similar profile to that observed in acidic buffer while the 1:3-CL formulation did not show size alterations when exposed to urine.

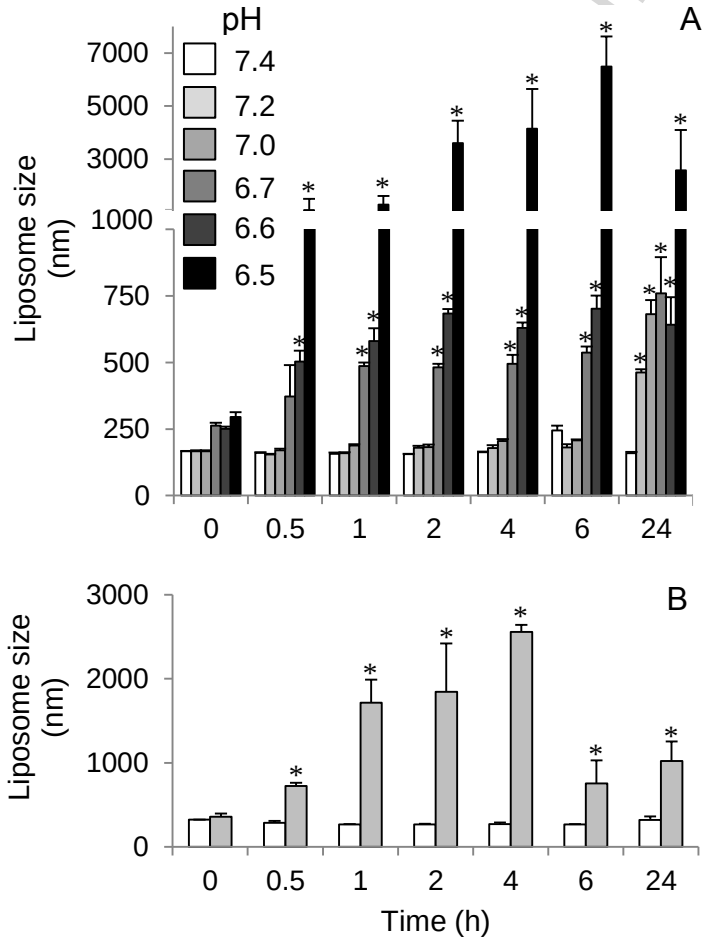

Figure 3. Time course of the size profile of 1:3-pH-RL in PBS at pH ranging from 7.4 to 6.5 (A) and of 1:3-CL (□) and 1:3-RL (■) in mouse urine (B) at 25 °C. Panel A: *p <0.05 refers to the formulation at specific time point *vs* time zero at the same pH; panel B: * p <0.05 refers to formulations incubated at pH 6.5 *vs* pH 7.4 at each time point.

Figures 4A, B and C report the long term stability profiles of all pH-responsive and control vesicles at pH 7.4. The size of CL remained approximately of 200 nm for 16 days regardless of the $mPEG_{5kDa}$-DSPE/Brij-700®/lipid molar ratio composition. The size of

the 0.2:0.6-pH-RL and 1:3-pH-RL formulations was stable up to 12 days and increased to approximately 500 nm after 16-20 days, while the size of 0.5:1.5-pH-RL increased to approximately 500 nm in 5 days.

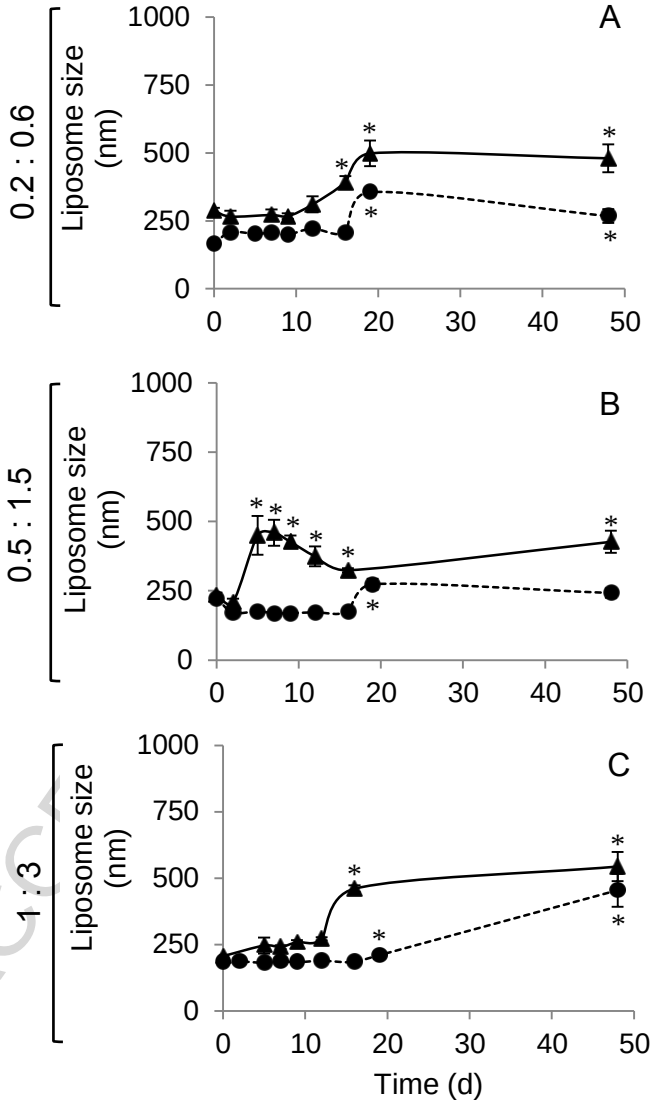

Figure 4. Time course of the size profile of pH-responsive liposomes (pH-RL: ▲) and control liposomes (CL: ●) for the 0.2:0.6-pH-RL and 0.2:0.6-CL formulations (A), 0.5:1.5-pH-RL and 0.5:1.5-CL formulations (B), and 1:3-pH-RL and 1:3-CL formulations (C) in PBS at pH 7.4 at 25 °C. * $p < 0.05$ refers to the formulation at specific time point *vs* time zero.

3.3. Liposome zeta potential in response to pH

At pH 7.4, the pH-RL liposomes displayed a negative zeta potential. Figure 5A shows that the absolute zeta potential value increased as the stearoyl-PEG-polySDM density on the liposome surface increased and significantly decreased to nearly neutrality when the liposomes were incubated at pH 6.5, regardless the composition.

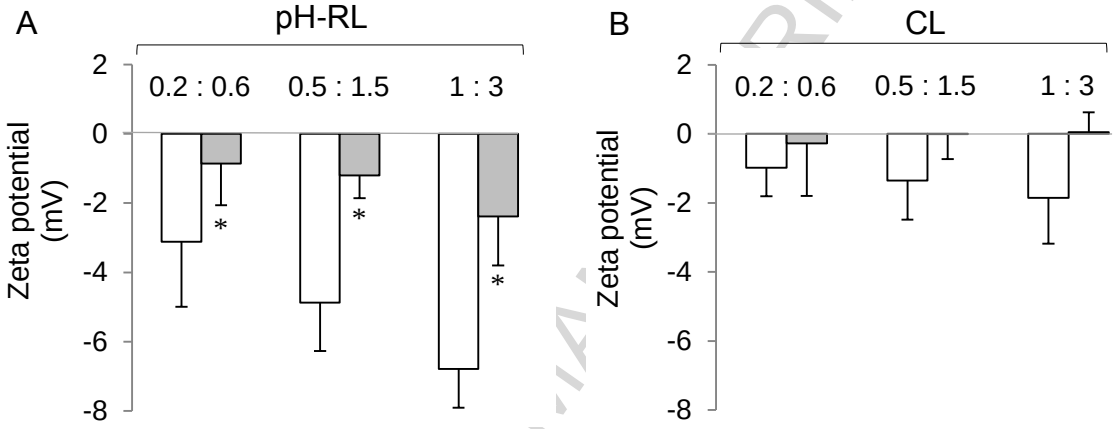

Figure 5. Zeta potential of the three pH-RL formulations (A) and CL formulations (B) in PBS at pH 7.4 (□) and 6.5 (■). * $p < 0.05$ refers to each formulation at pH 6.5 *vs* pH 7.4.

This behaviour was in fair agreement with the results reported in the literature for similar systems [48,49]. Figure 5B shows that the zeta potential of control liposomes reflected the neutral character of the Brij-700® on the vesicle surface. Indeed, CL formulations displayed nearly neutral zeta potential, regardless of the polymer/lipid composition and a slight decrease of the absolute values when the pH shifted from 7.4 to 6.5. The 1:3-pH-RL and 1:3-CL in mouse urine displayed a zeta potential value of -0.59 ± 0.35 and of 0.03 ± 0.45, respectively, confirming that the responsive liposomes possess a nearly neutral zeta potential in mouse urine.

3.4. TEM imaging of liposomes

The TEM images of pH-RL and CL at pH 7.4 and 6.5 reported in Figure 6 confirm the results obtained by DLS.

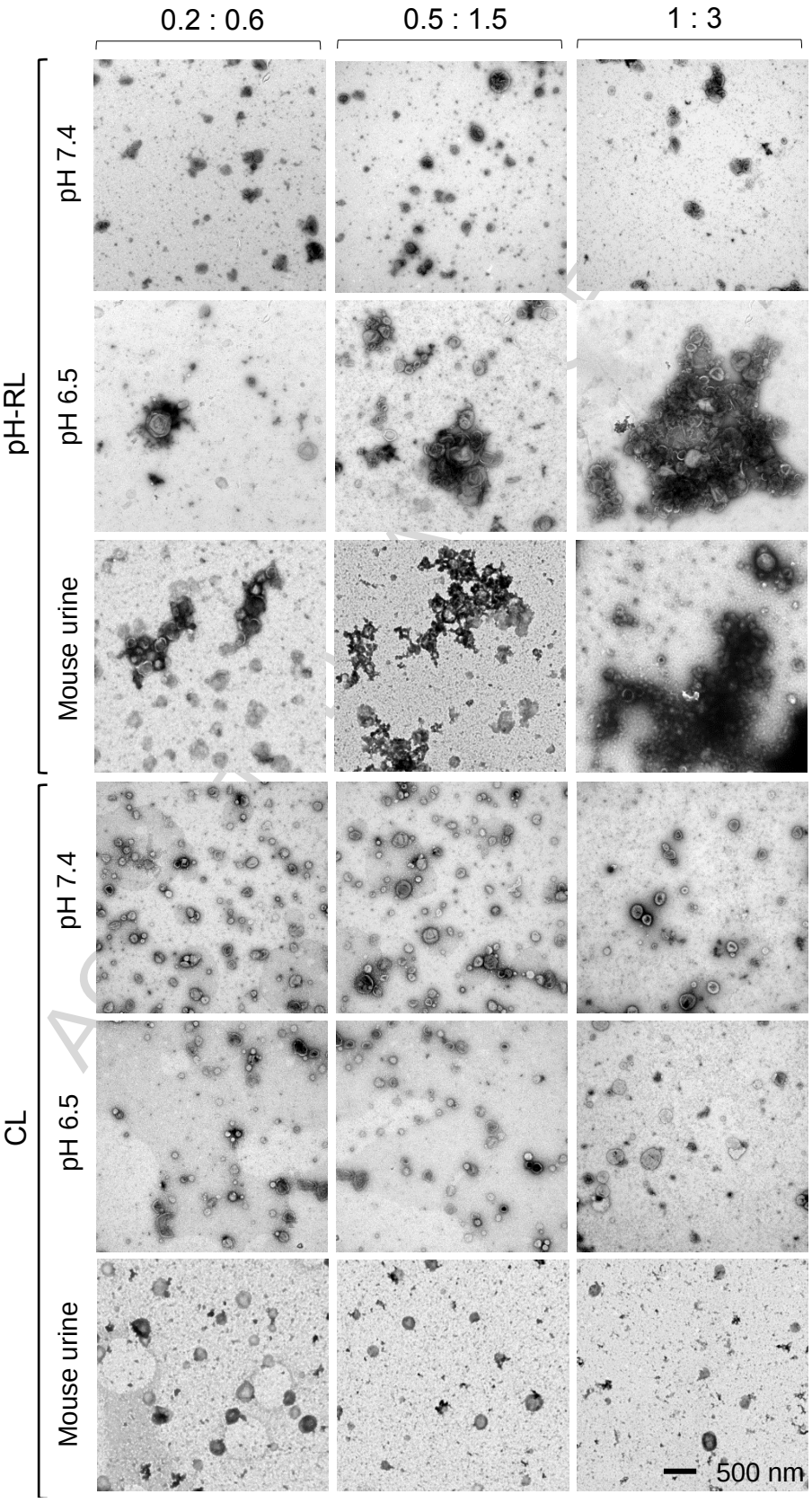

Figure 6. TEM images of the liposome formulations at pH 7.4, pH 6.5 and mouse urine. The $mPEG_{5kDa}$-DSPE/stearoyl-PEG-polySDM composition for pH-RL and the $mPEG_{5kDa}$-DSPE/Brij-700® composition for CL are reported on the top-line of the figure. The size bar corresponds to 500 nm.

At neutral pH, small separate pH-RL particles were observed. At acidic conditions, the vesicles underwent size increase and aggregation. As the stearoyl-PEG-polySDM density increased on the liposome surface, the formation of macroaggregates became more pronounced. Neither the particle size increase nor the aggregation was instead observed with CL at all tested surface Brij-700® densities and pH conditions.

3.5. Protein release

The protein release profiles reported in Figure 7 were obtained by liposome dialysis. The BSA release was negligible within the first 6 h of incubation irrespective of the pH and liposome composition. Approximately 50% of the loaded BSA was released in 24 h by the 0.2:0.6-CL and 0.2:0.6-pH-RL while all other liposome formulations released approximately 35% of the loaded BSA; however, the difference was not statistically significant. In any case, the BSA release was complete in about 10 days.

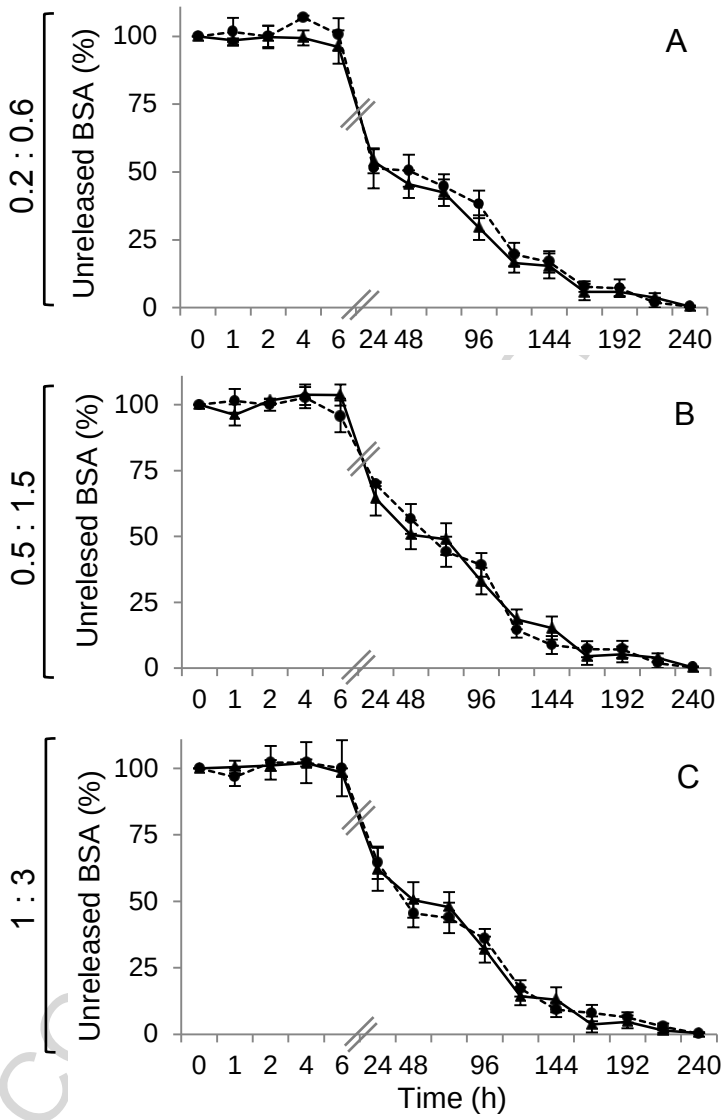

Figure 7. BSA release profiles from 0.2:0.6-pH-RL formulations (A), 0.5:1.5-pH-RL formulations (B), and 1:3-pH-RL (C) in PBS at pH 7.4 (▲) and 6.5 (●) at 25 °C. The BSA release at each time point at pH 7.4 *vs* pH 6.5 was not statistically different.

3.6. Interaction of liposomes with the cells

The pH-dependent ability of the pH-RL liposomes to associate to cells was investigated using bladder cancer cells (MB49) and macrophages, which are crucial modulators of the tumour microenvironment [50]. The study was carried out by flow cytometry and

confocal microscopy using double fluorescent 1:3-CL and 1:3-pH-RL formulations to trace both the protein and the carrier.

The cytofluorimetric data reported in Figure 8A and B show that after 6 h of incubation at pH 6.5 with 1:3-pH-RL, 57% of MB49 cells and 90% of THP-1-derived macrophages (TDM) were positive for BSA-loaded liposomes. The cell association of pH-RL at pH 7.4 was significantly lower than that observed at acidic pH for both cell lines. Non-responsive control liposomes yielded very low association at both pHs.

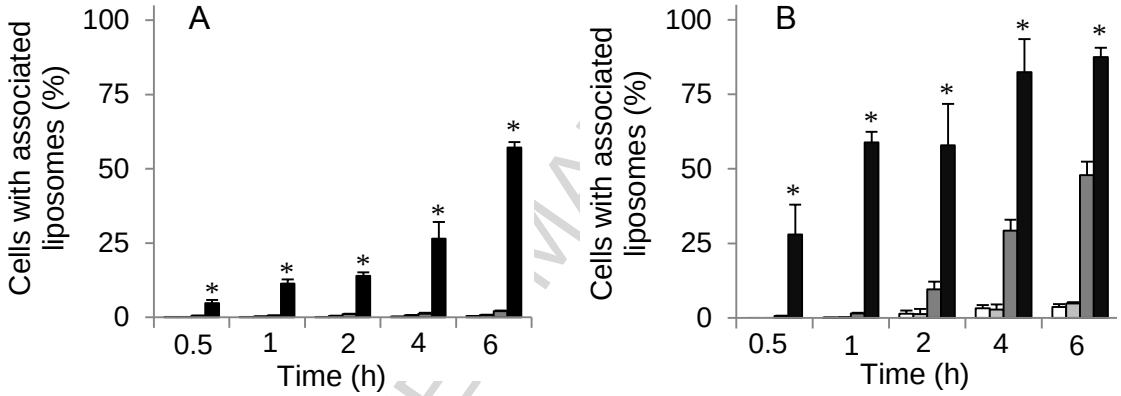

Figure 8. Time-dependent association of FITC-BSA-loaded rhodamine-DHPE liposomes to MB49 cells (A) and TDM (B): incubation was performed with 1:3-CL at pH 7.4 (□) and 6.5 (■) and with 1:3-pH-RL formulations at pH 7.4 (■) and 6.5 (■). * $p < 0.05$ refers to pH-RL at pH 6.5 *vs* pH 7.4 at each time point.

Confocal microscopy showed the localization of the pH-sensitive FITC-BSA-loaded liposomes at the cellular level and confirmed the cytofluorimetric data. The pH-RL liposomes associated more rapidly to TDM cells than to MB49 cells, and the association was favoured by the acidic pH. Figure 9A and B show that after 6 h of incubation, the liposomes were detected inside the TDM cells, probably within the phagosomes, whereas they remained associated to the plasma membrane of MB49 cells. These results were confirmed by line-scanning analysis of cells (Figure 9C and E). The results reported in Figure 9D and F of the double stained pH-RL liposomes associated to a single cell definitively confirmed that TDM cells internalized the liposomes more efficiently than

MB49, and the pH-RL liposomes association profile in both cell lines was significantly favoured by acidic pH.

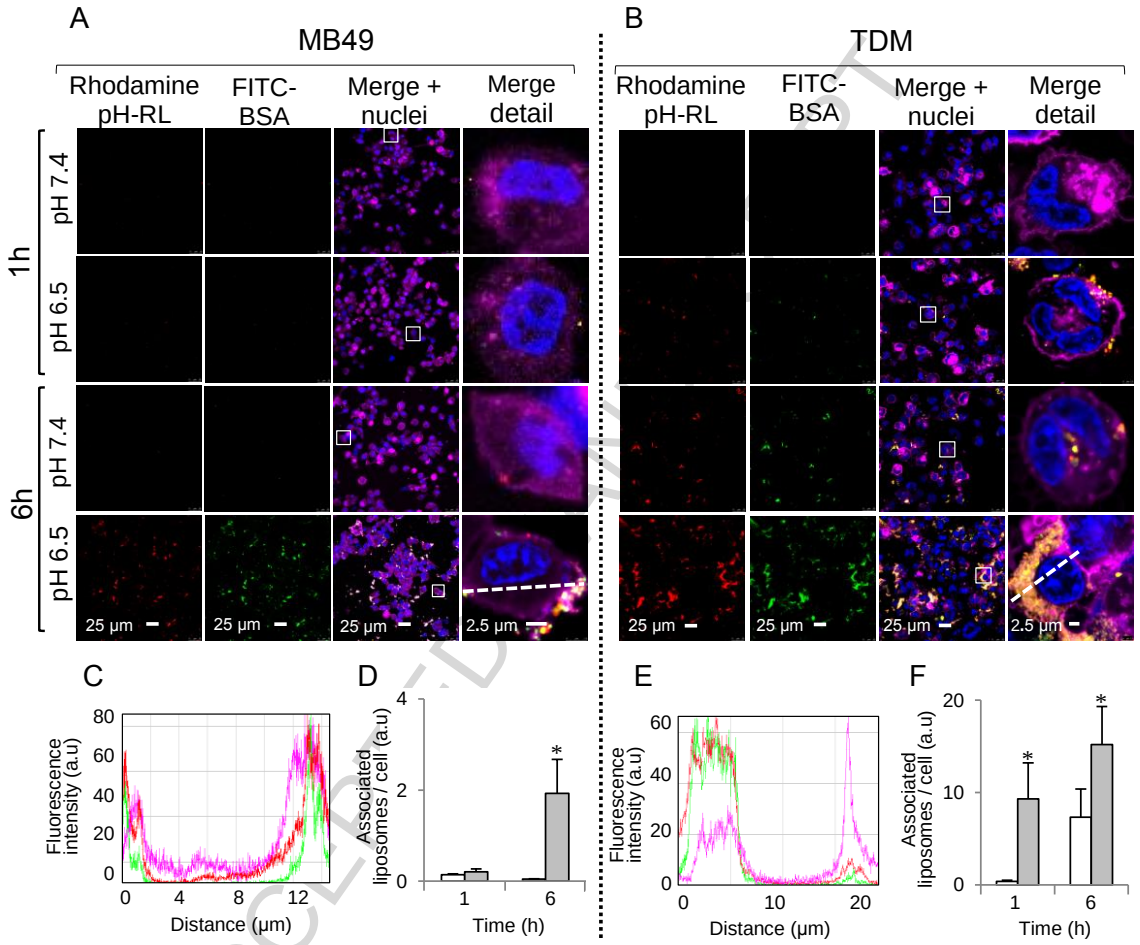

Figure 9. Confocal microscopy images of MB49 cells (A) and TDM (B) treated with 0.5 mg/mL of FITC-BSA-loaded rhodamine-DHPE labelled 1:3-pH-RL at pH 7.4 and 6.5 for 1 h (upper panels) and 6 h (lower panels). The images were acquired using the 580 nm channel for rhodamine-DHPE detection (red), the 525 nm channel for FITC-BSA detection (green), the 461 nm channel for nuclei detection (blue), and the 660 nm channel for cell membrane detection (purple). The yellow signal results from merging the red and green signals. A magnified image from the merging is shown in the last column of each panel. The localization of liposomes (red profile), BSA (green profile) and cell membrane (purple profile), reported in panel C and E, was determined by line-scanning analysis along the white dotted axis in the merged bottom right images of panel A and B. The quantification of the red and green co-localized signals per MB49 cell (D) and TDM cell

(F) was obtained from images of cells incubated at pH 7.4 (□) and 6.5 (■) and expressed as arbitrary unit (a.u.). At least 10 fields (with an average of 80 cells per field) were analysed per each condition. * $p < 0.05$ refers to pH-RL at pH 6.5 *vs* pH 7.4 at each time point.

Finally, neither significant cell association nor protein delivery was observed with CL liposomes at all experimental incubation times and pH (supplementary Figure S4).

3.7. *In vivo* studies

The ability of pH-responsive liposomes to bind the bladder epithelium was evaluated by intra-bladder instillation to mice of FITC-BSA-loaded rhodamine-DHPE labelled 1:3-pH-RL or 1:3-CL. Figure 10 reports representative confocal fluorescence microscopy images of a cross-section of the bladder of a mouse treated with pH-RL at pH 6.5. The white square in panel A highlights the region magnified in panels B-D where the liposomes appear massively associated to the bladder epithelium. The yellow labelled tissue areas in panels A and B result from merging the fluorescent signals of FITC-BSA and rhodamine-labelled pH-RL.

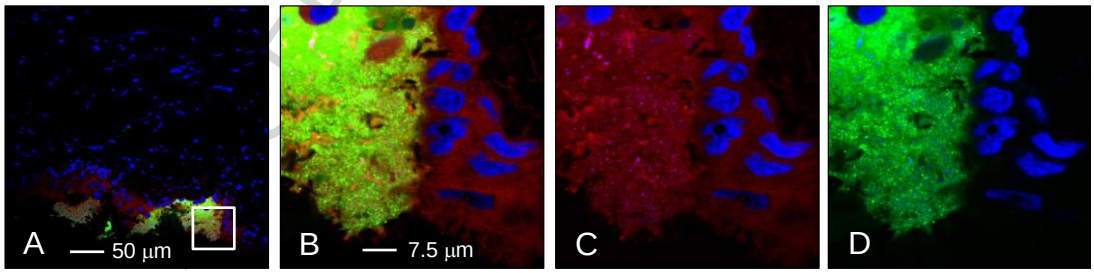

Figure 10. Microscopic examination of mice bladder cross-sections after installation of FITC-BSA-loaded Rhodamine-DHPE labelled liposomes (1:3-pH-RL) at pH 6.5. The nuclei were stained with DAPI, and the tissue was analysed by confocal fluorescence microscopy. The images were acquired using the 580 nm channel for rhodamine-DHPE detection (red), the 525 nm for FITC-BSA detection (green) and the 461 nm channel for nuclei detection (blue). The yellowish-green signal results from merging the red and green signal (panel A and B). A magnified image of the white square of image A is

shown in panel B and the corresponding green channel and red channel are depicted in panel C and D, respectively.

The histological analysis of a 4 μm thick bladder cross-section showed that the pH-responsive liposome aggregates span a quite large epithelium surface. No liposomal association to the bladder epithelium was detected when pH-RL was administered at pH 7.4 or when CL was injected into the mice bladders at pH 7.4 and 6.5 (data not shown).
The results showed that the pH-RL efficiently deliver BSA to the epithelium when inoculated in the mouse bladder at pH 6.5.

4. Discussion

The study was inspired by the need to provide a prolonged exposure of the bladder epithelium to the biotherapeutics currently under investigation, such as IFN-α and HP-NAP of *Helicobacter pylori* [4,7], upon local instillation. The pH sensitive pH-RL liposomes described here were designed to respond to the conditions of the bladder lumen with the aim to enhance the liposome bioadhesion and the delivery of biotherapeutic payloads to the bladder epithelium by preventing the rapid drug clearance due to bladder emptying.
The pH sensitive liposomes were obtained by decoration with a stearoyl-PEG-polySDM moiety, which was previously demonstrated to reversibly switch from the hydrophilic to the hydrophobic state by pH changes in the physiopathological range conditions [38]. The stearoyl-PEG-polySDM bioconjugate containing 7 methacryloyl sulfadimethoxine monomers was considered suitable to the aim of the work since it is responsive to the urine pH. Indeed, the hepta-SDM stearoyl-PEG conjugate has an apparent pK_a of 7.2, which yields a LogD of 15.00 and 17.87 at pH 7.4 and pH 6.5, respectively [48], and 4.3 and 1 charged SDM monomers on each stearoyl-PEG-polySDM unimer at 7.4 and 6.5, respectively. Therefore, the pH decrease from pH 7.4 to 6.5 results in an uncharged hydrophobic liposome surface. The composition of the liposomes was selected on the basis of previous results [51]. This study showed that the addition of $mPEG_{5kDa}$-DSPE enhanced the overall liposome stability at pH 7.4, which is a requisite for their storing and handling. Brij-700® was selected to produce control stealth liposomes in virtue of its

non-charged feature and hydrophilicity (LogP 9.09) in a wide physiological pH range and its comparable length to the stearoyl-PEG-polySDM copolymer.

The protein loading capacity and efficiency preliminarily investigated to select suitable conditions to load a protein model (BSA) in liposomes were in fair agreement with the literature: the loading capacity increased and the efficiency decreased as the protein/lipid w/w feed ratio increased [47]. The liposome formulation obtained at 10 mg/mL lipid and rehydrated with 1 mg/mL BSA containing buffer was finally selected, taking into account the liposome extrusion process feasibility, and to balance the protein loading and the time required for the removal of non-loaded protein by dialysis.

The liposome decoration with $mPEG_{5kDa}$-DSPE and stearoyl-PEG-polySDM did not alter the loading capacity or the lipid bilayer permeability. However, both the protein loading and the surface decoration with the polymers affected the liposome size. The $mPEG_{5kDa}$-DSPE- and stearoyl-PEG-polySDM-decorated BSA-loaded formulations displayed a slightly larger size than their non-BSA loaded (BSA-free) counterparts described in our previous work [38]. The effect of the polymer decoration, already observed with similar formulations [47], may be ascribed to a different rearrangement of the lipid bilayer with embedded BSA, which can slightly affect the curvature of the liposomes. On the other hand, similar to what has been reported in the literature [52-54], the size of liposomes slightly decreased upon PEG decoration, probably as consequence of the dynamic structural rearrangement of the lipid bilayer.

The zeta potential and size analysis studies (DLS and TEM) performed to evaluate the response of the liposomes when exposed to bladder-mimicking conditions (pH 6.5) highlighted the effect of the poly-SDM blocks of the pH-responsive polymer in controlling the colloidal properties of liposomes by pH changes. The environmental pH dictated the surface charge of pH-RL, while it had no effect on naked (data not shown) or CL liposomes. Indeed, these liposomes displayed an overall negative charge at pH 7.4, a condition that ensures repulsion and colloidal stability of the liposomes. The protonation of the sulfonamide group of the methacryloyl sulfadimethoxine monomers on the liposome surface at pH 6.5 remarkably decreased the zeta potential absolute value. The charge loss yielded a reduction of the repulsion forces and induced a hydrophobic liposome surface which, together, mediated the liposome aggregation and size

enlargement due to the formation of inter-vesicle intermingles involving the hydrophobic polySDM blocks. Inter-vesicle hydrophobic interactions of the polySDM blocks overcome residual anionic repulsive forces at pH 6.5. On the other hand, the Brij-700® used in control liposomes possesses a non-ionisable hydrophilic feature (LogP 9.09), which inhibits liposome aggregation by obstruction and steric repulsion, regardless the pH [55]. The size enlargement started soon after the pH was decreased from 7.4 to 6.5 and achieved a plateau after approximately 1-2 h. The increase of the liposome PDI, a descriptor of the macroscopic response of the vesicles, at pH 6.5 indicates that, under these conditions, the lipid carrier underwent a heterogeneous macro-aggregation rearrangement. The TEM analysis confirmed that at an acidic pH (PBS at pH 6.5) and in urine the pH-RL underwent aggregation, which was directly proportional to the surface density of the poly-SDM blocks. According to the apparent poly-SDM pKa [56], the calculated percentage of charged SDM monomers at pH 7.4 and 6.5 was 61% and 14%, respectively. Consequently, the protonation and aggregation degree of pH-RL was found to increase as the pH stepwise decreased from 7.4 to 6.5. At pH 7.0 the pH-responsive liposomes underwent slower aggregation than at pH 6.5 (Figure 3A). The 6 h lag time before liposome aggregation observed at pH 7.0 can be ascribed to a lower LogD and higher charged/deprotonated ratio of methacryloyl sulfadimethoxine monomers than that calculated at pH 6.5, which slightly reduces the inter-vesicle intermingles involving the poly-SDM blocks.

Because pH-RLs were designed for local instillation into the bladder, their structural behaviour when exposed to mouse urine was investigated. In urine, the aggregation of the liposomes showed a similar profile to that observed in PBS at 6.5 with a fast liposome size increase, indicating that the urine pH triggers the liposome association and the urine components do not inhibit the liposome response to the acidic environment. Furthermore, the aggregation profile of pH-responsive liposomes in mouse urine at pH 7.0 [57], was found to be more rapid compared to PBS at the same pH. Notably, mouse urine possesses a quite higher osmolality (2,317 ± 80 mOsmol/kg H_2O) [58] with respect to PBS (280 - 315 mOsm/kg H_2O), which may favour hydrophobic interactions of the polySDM blocks on the liposome surface and thus a more rapid liposome aggregation under the same pH conditions. The aggregation was not observed for the control liposomes due to

permanently hydrophilic non-charged surface that provides for obstruction and steric repulsion at all pH tested [55]. The size reduction of liposomes observed at 6 h and 24 h in urine may be ascribed to the pH increase of urine that occurs over time [59]; such an increase promotes deprotonation of methacryloyl sulfadimethoxine monomers and partial liposome dissociation due to repulsive charges.

The pH-RL and CL formulations showed good stability at pH 7.4 for up to 12 days without significant size or PDI alteration. Instability for both formulations at 12 days was quite similar and may occur because of the polymer detachment from the liposome bilayer over time. Only the 0.5:1.5-pH-RL formulation displayed an earlier size increase after 3 days. This may be ascribed to insufficient stearoyl-PEG-polySDM density to ensure adequate anionic charges (zeta potential is -5 mV) and repulsive forces at pH 7.4. Nevertheless, the stearoyl-PEG-polySDM density on the 0.5:1.5-pH-RL allows for sufficiently strong hydrophobic inter-vesicle interactions, the latter being instead too poor in the 0.2:0.6-pH-RL that have a lower polymer density. The liposomes showed similar long term stability profiles at 25 °C and 37°C. This behaviour can be explained by the fact that the lipid mixture used to produce the liposomes (soy phosphatidylcholine/cholesterol) possesses a low transition temperature (range -21°C to -18 °C) [60], and thus the lipid bilayers are in the fluid state at both temperatures tested while the polymers behave similarly at the two temperatures.

The protein release profile from the pH-RL formulations at 25 °C showed that neither the polymer coating nor the pH of incubation affected the release, thus, neither the liposome aggregation nor the structural changes of the polySDM blocks induced by acidic conditions significantly altered the membrane permeability of the vesicles. Furthermore, the protein release occurred in 10 days after 6 h lag time, allowing the carrier to associate to the biological target surface before a prolonged release takes place. According to the literature, the absence of burst release of BSA may be correlated to both interaction of the protein with the lipid components of the liposome bilayer and the low permeability of BSA through the lipid bilayer [61]. No significant difference in the BSA release profile was observed at 37 °C, which may be correlated to the fact that the lipid mixture used to prepare the liposomes is in a fluid state at both temperatures and the bilayer permeability does not change significantly between 25 °C and 37 °C [60].

Based on the stability profile at neutral pH and the responsive behaviour to the intra-bladder pH [40], the 1:3:100 $mPEG_{5kDa}$-DSPE/stearoyl-PEG-polySDM/lipids molar ratio formulation was selected for the *in vitro* and *in vivo* biological studies.

The association of the BSA-loaded liposomes was tested *in vitro* on MB49 urothelial carcinoma cells and PMA-differentiated THP-1 macrophages that do not possess a specific functional profile [62]. The MB49 cell line is an excellent model to study anti-tumour agents [63]. Macrophages are crucial cells involved in the control of tumour progression [50]. Monocytes and macrophages are in fact recruited from the circulation into the tumours, where they actively participate to the carcinogenic process. Tumour-associated macrophages have been related with poor clinical outcomes [50], while macrophage activation enhances the anti-tumour immune responses [64]. Studies performed to yield macrophage targeting have shown that the liposome uptake by macrophages depends on a variety of features, including size, charge and composition [65], although the macrophage heterogeneity has not allowed to extensively elucidate the impact of liposome features on the immune response [64,66]. We focused our investigation on assessing whether pH-RL underwent association to and engulfment by macrophages.

The cytofluorimetric data showed that the association of pH-RL to both cell lines was remarkably higher in acidic conditions mimicking the urine than at pH 7.4. Under the acidic conditions in fact, the liposome surface charge is significantly decreased (absolute zeta potential decrease) and the surface hydrophobicity increases (LogD decrease); hence, the liposome aggregation and association with cells may occur. The pH-sensitive liposome association to macrophages at pH 7.4 may result from the surface anionic charges that the vesicles possess at this pH; in fact, negatively charged liposomes have been reported to be taken up at some extent by macrophages [65].

The confocal microscopy images showed that the uptake of the BSA-loaded liposomes by MB49 cancer cells at pH 7.4 over time was negligible, confirming that under these conditions their colloidal stability and surface charge inhibited the adhesion to the cells due to the anionic repulsive charges of pH-RL and cells. On the contrary, at pH 6.5, pH-RL bound to the cell surface. Even though the cell interaction resulted in limited distribution of pH-RL in the cytoplasm, the association of carriers to epithelial cells may

represent a valuable advantage for the delivery of therapeutic proteins because it can increase their residence time and their local and gradual release.

The more pronounced and faster pH-RL association to the macrophages with respect to the MB49 cancer cells observed at both pHs can be ascribed to the phagocytic activity of macrophages. Notably, at acidic pH, the overall association efficiency of the pH-RL with macrophages was significantly higher with respect to both neutral conditions and to what was observed for bladder cancer cells. Moreover, after a longer exposure time, liposomes accumulated in the cytoplasm.

The intracellular protein delivery and release from this family of carriers can offer significant therapeutic advantages by potentiating the activation of immune cells. Indeed, the delivery of therapeutic molecules to macrophages by targeted liposomes is a very prolific field of investigation for the treatment of a variety of diseases, including cancer [29,65]. We recently discovered that a bacterial protein, namely HP-NAP, has a key role in driving a T helper (Th) 1 immune response upon binding to the Toll-like Receptor 2 (TLR2) [67]. Although TLR2 is mainly located on the surface of innate immune cells (i.e., macrophages, dendritic cells), an intracellular localization has also been described. Macrophages (both the THP-1 cell line [68] and the human-derived macrophages [69]) are among the cells where intracellular TLR2 has been found. Dedicated studies are required to further elucidate the fate of the liposome-encapsulated therapeutic protein and whether it is efficiently released from the phagocytized lipid carriers in its biologically active form.

The bioadhesion to the cells as a result of the surface hydrophobic conversion and aggregation of pH-RL at acidic pH was recapitulated *in vivo* upon instillation of the nanocarrier in the mouse bladder. The pH-responsive liposomes at pH 6.5 were administered 1 min after pH setting when liposomes were in the non-aggregated state (time 0 in Figure 2E). This approach ensured the catheter was not clogged by pH-responsive liposome aggregates and aggregation takes place within the bladder. This, in turn, yielded an efficient delivery of loaded BSA compared to the CL instilled in the bladder at the same acidic pH. pH-RL remained associated to the bladder surface even after washing, proving that association of the BSA-loaded carrier to the epithelium is quite robust. On the other hand, while the BSA-loaded carrier remained localized on the

urothelium, we also observed the fluorescent label used to tag liposomes (rhodamine-DHPE) in the deeper cellular layers of the epithelium, suggesting that partial liposome dissociation occurred upon adhesion.

Bioadhesion is conveyed to drug delivery systems in all the circumstances in which a prolonged contact with biological surfaces is desired to increase the local site exposure to the loaded drug [70]. According to the evidence, the combination of the hydrophobic/neutral conversion of the liposome surface and their macroscopic aggregation under the bladder acidic conditions control the deposition of the carrier on the bladder surface, thus enhancing the protein disposition in bladder tissue.

5. Conclusions

The results reported in this work show that the decoration of BSA-loaded liposomes with the pH-responsive polymer stearoyl-PEG-polySDM provides a vehicle that efficiently associates with and delivers the protein payload to cancer cells and macrophages under conditions mimicking the bladder environment. This "smart" nanocarrier represents a proof-of-concept, and it has been explored for the delivery of biologics to the bladder epithelium. While the liposomes are colloidally stable at neutral pH, they are "activated" when exposed to the acid environment of the bladder, yielding epithelium adhesion. The liposome adhesion to the urothelium would ensure enhanced protein disposition at this site as well as interaction with macrophages that are involved in the control cancer growth, offering a clear advantage for bladder cancer therapy.

Recently, proteins from bacteria have been shown to remarkably inhibit bladder cancer growth *in vivo* due to the specific activation of macrophages. However, these proteins require proper delivery strategies to ensure adequate urothelium exposure upon local administration.

On-going studies are investigating the therapeutic effect of pH-RL loaded with immunostimulating proteins for the treatment of bladder cancer using an ectopic tumour model. Detailed investigations will elucidate the mechanism of action and the immunostimulating potency of the biotherapeutic loaded pH-RL with respect to the unformulated proteins.

Acknowledgements

We acknowledge the University of Padova for financial support through the "Progetto di Ricerca di Ateneo" (grant N° CPDA121714; CUP C94H12000020005) funding schemes. MdB was supported by "Associazione Italiana per la Ricerca sul Cancro/Fondazione Cariparo" and "Progetti di Ricerca di Ateneo" (grant N° CPDA137871). MVC was recipient of a research fellowship granted by "Fondazione Cariplo" (grant N° 2011-0485).

References

[1] L.A. Torre, F. Bray, R.L. Siegel, J. Ferlay, J. Lortet-Tieulent, A. Jemal, Global cancer statistics, 2012, CA: a Cancer Journal for Clinicians. 65 (2015) 87–108.

[2] S.F. Shariat, D.C. Chade, P.I. Karakiewicz, D.S. Scherr, G. Dalbagni, Update on intravesical agents for non-muscle-invasive bladder cancer, Immunotherapy. 2 (2010) 381–392.

[3] D.R. Yates, M. Rouprêt, Failure of bacille Calmette-Guérin in patients with high risk non-muscle-invasive bladder cancer unsuitable for radical cystectomy: an update of available treatment options, BJU International. 106 (2010) 162–167.

[4] D. Lamm, M. Brausi, M.A. O'Donnell, J.A. Witjes, Interferon alfa in the treatment paradigm for non–muscle-invasive bladder cancer, Urologic Oncology: Seminars and Original Investigations. 32 (2014) 35.e21–35.e30.

[5] P. Sidaway, Bladder cancer: atezolizumab effective against advanced-stage disease, Nat Rev Urol. 13 (2016) 238–238.

[6] C. Sänger, A. Busche, G. Bentien, R. Spallek, F. Jonas, A. Böhle, M. Singh, S. Brandau, Immunodominant PstS1 antigen of mycobacterium tuberculosis is a potent biological response modifier for the treatment of bladder cancer, BMC Cancer. 4 (2004) 86.

[7] G. Codolo, M. Fassan, F. Munari, A. Volpe, P. Bassi, M. Rugge, F. Pagano, M.M. D'Elios, M. de Bernard, HP-NAP inhibits the growth of bladder cancer in

mice by activating a cytotoxic Th1 response, Cancer Immunology, Immunotherapy. 61 (2011) 31–40.

[8] D.-S. Hsieh, H. Wang, S.-W. Tan, Y.-H. Huang, C.-Y. Tsai, M.-K. Yeh, C.J. Wu, The treatment of bladder cancer in a mouse model by epigallocatechin-3-gallate-gold nanoparticles, Biomaterials. 32 (2011) 7633–7640.

[9] C. Mugabe, Y. Matsui, A.I. So, M.E. Gleave, J.H.E. Baker, A.I. Minchinton, I. Manisali, R. Liggins, D.E. Brooks, H.M. Burt, In vivo evaluation of mucoadhesive nanoparticulate docetaxel for intravesical treatment of non-muscle-invasive bladder cancer, Clinical Cancer Research. 17 (2011) 2788–2798.

[10] E. Bilensoy, C. Sarisozen, G. Esendağlı, A.L. Doğan, Y. Aktaş, M. Şen, N.A. Mungan, Intravesical cationic nanoparticles of chitosan and polycaprolactone for the delivery of Mitomycin C to bladder tumors, International Journal of Pharmaceutics. 371 (2009) 170–176.

[11] C. Mugabe, P.A. Raven, L. Fazli, J.H.E. Baker, J.K. Jackson, R.T. Liggins, A.I. So, M.E. Gleave, A.I. Minchinton, D.E. Brooks, H.M. Burt, Tissue uptake of docetaxel loaded hydrophobically derivatized hyperbranched polyglycerols and their effects on the morphology of the bladder urothelium, Biomaterials. 33 (2012) 692–703.

[12] C. Le Visage, N. Rioux-Leclercq, M. Haller, P. Breton, B. Malavaud, K. Leong, Efficacy of paclitaxel released from bio-adhesive polymer microspheres on model superficial bladder cancer, The Journal of Urology. 171 (2004) 1324–1329.

[13] Z. Lu, T.-K. Yeh, M. Tsai, J.L.-S. Au, M.G. Wientjes, Paclitaxel-loaded gelatin nanoparticles for intravesical bladder cancer therapy, Clinical Cancer Research. 10 (2004) 7677–7684.

[14] Z. Lu, T.-K. Yeh, J. Wang, L. Chen, G. Lyness, Y. Xin, M.G. Wientjes, V. Bergdall, G. Couto, F. Alvarez-Berger, C.E. Kosarek, J.L. Au, Paclitaxel gelatin nanoparticles for intravesical bladder cancer therapy, The Journal of Urology. 185 (2011) 1478–1483.

[15] J.M. McKiernan, L.J. Barlow, M.A. Laudano, M.J. Mann, D.P. Petrylak, M.C.

Benson, A phase I trial of intravesical nanoparticle albumin-bound paclitaxel in the treatment of bacillus Calmette-Guérin refractory nonmuscle invasive bladder cancer, The Journal of Urology. 186 (2011) 448–451.

[16] J.W. Johnson, R. Nayar, J.J. Killion, A.C. von Eschenbach, I.J. Fidler, Binding of liposomes to human bladder tumor epithelial cell lines: implications for an intravesical drug delivery system for the treatment of bladder cancer, Selective Cancer Therapeutics. 5 (1989) 147–155.

[17] D. Christensen, K.S. Korsholm, P. Andersen, E.M. Agger, Cationic liposomes as vaccine adjuvants, Expert Review of Vaccines. 10 (2014) 513–521.

[18] L. Liguori, B. Marques, A. Villegas-Mendez, R. Rothe, J.-L. Lenormand, Liposomes-mediated delivery of pro-apoptotic therapeutic membrane proteins, Journal of Controlled Release. 126 (2008) 217–227.

[19] J. Regberg, A. Srimanee, Ü. Langel, Applications of cell-penetrating peptides for tumor targeting and future cancer therapies, Pharmaceuticals. 5 (2012) 991–1007.

[20] I. Eue, Growth inhibition of human mammary carcinoma by liposomal hexadecylphosphocholine: Participation of activated macrophages in the antitumor mechanism, International Journal of Cancer. 92 (2001) 426–433.

[21] H. Zhuo, Y. Peng, Q. Yao, N. Zhou, S. Zhou, J. He, Y. Fang, X. Li, H. Jin, X. Lu, Y. Zhao, Tumor imaging and interferon-γ-inducible protein-10 gene transfer using a highly efficient transferrin-conjugated liposome system in mice, Clinical Cancer Research. 19 (2013) 4206–4217.

[22] L. Wang, W. Su, Z. Liu, M. Zhou, S. Chen, Y. Chen, D. Lu, Y. Liu, Y. Fan, Y. Zheng, Z. Han, D. Kong, J.C. Wu, R. Xiang, Z. Li, CD44 antibody-targeted liposomal nanoparticles for molecular imaging and therapy of hepatocellular carcinoma, Biomaterials. 33 (2012) 5107–5114.

[23] M.S. Muthu, D.T. Leong, L. Mei, S.-S. Feng, Nanotheranostics - application and further development of nanomedicine strategies for advanced theranostics, Theranostics. 4 (2014) 660–677.

[24] S. Jain, V. Mishra, P. Singh, P.K. Dubey, D.K. Saraf, S.P. Vyas, RGD-anchored magnetic liposomes for monocytes/neutrophils-mediated brain targeting,

International Journal of Pharmaceutics. 261 (2003) 43–55.

[25] F. Hajos, B. Stark, S. Hensler, R. Prassl, W. Mosgoeller, Inhalable liposomal formulation for vasoactive intestinal peptide, International Journal of Pharmaceutics. 357 (2008) 286–294.

[26] H. Epstein-Barash, D. Gutman, E. Markovsky, G. Mishan-Eisenberg, N. Koroukhov, J. Szebeni, G. Golomb, Physicochemical parameters affecting liposomal bisphosphonates bioactivity for restenosis therapy: internalization, cell inhibition, activation of cytokines and complement, and mechanism of cell death, Journal of Controlled Release. 146 (2010) 182–195.

[27] G. Gregoriadis, Liposomes in the therapy of lysosomal storage diseases, Nature. 275 (1978) 695–696.

[28] R. Thekkedath, A. Koshkaryev, V.P. Torchilin, Lysosome-targeted octadecyl-rhodamine B-liposomes enhance lysosomal accumulation of glucocerebrosidase in Gaucher's cells in vitro, Nanomedicine. 8 (2013) 1055–1065.

[29] A. Nardin, M. Lefebvre, K. Labroquere, O. Faure, J. Abastado, Liposomal muramyl tripeptide phosphatidylethanolamine: targeting and activating macrophages for adjuvant treatment of osteosarcoma, Current Cancer Drug Targets. 6 (2006) 123–133.

[30] J. Miyazaki, H. Nishiyama, I. Yano, A. Nakaya, H. Kohama, K. Kawai, A. Joraku, T. Nakamura, H. Harashima, H. Akaza, The therapeutic effects of R8-liposome-BCG-CWS on BBN-induced rat urinary bladder carcinoma, Anticancer Res. 31 (2011) 2065–2071.

[31] P. Tyagi, M. Kashyap, H. Hensley, N. Yoshimura, Advances in intravesical therapy for urinary tract disorders, Expert Opin Drug Deliv. 13 (2016) 71–84.

[32] J.B. Bassett, J.R. Tacker, R.U. Anderson, D. Bostwick, Treatment of experimental bladder cancer with hyperthermia and phase transition liposomes containing methotrexate, The Journal of Urology. 139 (1988) 634–636.

[33] R. Bachor, E. Reich, K. Miller, A. Rück, R. Hautmann, Photodynamic efficiency of liposome-administered tetramethyl hematoporphyrin in two human bladder cancer cell lines, Urol. Res. 23 (1995) 151–156.

[34] K.M. Peters, D. Hasenau, K.A. Killinger, M.B. Chancellor, M. Anthony, J.

Kaufman, Liposomal bladder instillations for IC/BPS: an open-label clinical evaluation, International Urology and Nephrology. 46 (2014) 2291–2295.

[35] J. Nirmal, P. Tyagi, M.B. Chancellor, J. Kaufman, M. Anthony, D.D. Chancellor, Y.T. Chen, Y.C. Chuang, Development of potential orphan drug therapy of intravesical liposomal tacrolimus for hemorrhagic cystitis due to increased local drug exposure, The Journal of Urology. 189 (2013) 1553–1558.

[36] J.J. Janicki, M.A. Gruber, M.B. Chancellor, Intravesical liposome drug delivery and IC/BPS, Transl Androl Urol. 4 (2015) 572–578.

[37] B. Kishor, M. Munira, K. Suvarna, K. Swapan, Intravesical drug delivery system for bladder: an overview, Ijpcbs. 3 (2014) 680–691.

[38] S. Bersani, M. Vila-Caballer, C. Brazzale, M. Barattin, S. Salmaso, pH-sensitive stearoyl-PEG-poly(methacryloyl sulfadimethoxine) decorated liposomes for the delivery of gemcitabine to cancer cells, European Journal of Pharmaceutics and Biopharmaceutics. 88 (2014) 670–682.

[39] I.F. Tannock, D. Rotin, Acid pH in tumors and its potential for therapeutic exploitation, Cancer Research. 49 (1989) 4373–4384.

[40] C. Rose, A. Parker, B. Jefferson, E. Cartmell, The Characterization of feces and urine: a review of the literature to inform advanced treatment technology, Critical Reviews in Environmental Science and Technology. 45 (2015) 1827–1879.

[41] S.-J. Jiang, L.-Y. Ye, F.-H. Meng, Comparison of intravesical bacillus Calmette-Guerin and mitomycin C administration for non-muscle invasive bladder cancer: A meta-analysis and systematic review, Oncol Lett. 11 (2016) 2751–2756.

[42] M.A. Pérez-Jacoiste Asín, M. Fernández-Ruiz, F. López-Medrano, C. Lumbreras, A. Tejido, R. San Juan, A. Arrebola-Pajares, M. Lizasoain, S. Prieto, J.M. Aguado, Bacillus Calmette-Guérin (BCG) infection following intravesical BCG administration as adjunctive therapy for bladder cancer: incidence, risk factors, and outcome in a single-institution series and review of the literature, Medicine (Baltimore). 93 (2014) 236–254.

[43] S. Bersani, S. Salmaso, F. Mastrotto, E. Ravazzolo, A. Semenzato, P. Caliceti, Star-Like Oligo-Arginyl-Maltotriosyl derivatives as novel cell-penetrating enhancers for the intracellular delivery of colloidal therapeutic systems,

Bioconjugate Chemistry. 23 (2012) 1415–1425.

[44] A.D. Bangham, M.M. Standish, J.C. Watkins, Diffusion of univalent ions across the lamellae of swollen phospholipids, Journal of Molecular Biology. 13 (1965) 238–IN27.

[45] J.P. May, M.J. Ernsting, E. Undzys, S.-D. Li, Thermosensitive liposomes for the delivery of gemcitabine and oxaliplatin to tumors, Molecular Pharmaceutics. 10 (2013) 4499–4508.

[46] M.B. Maeß, B. Wittig, A. Cignarella, S. Lorkowski, Reduced PMA enhances the responsiveness of transfected THP-1 macrophages to polarizing stimuli, Journal of Immunological Methods. 402 (2014) 76–81.

[47] X. Xu, A. Costa, D.J. Burgess, Protein encapsulation in unilamellar liposomes: high encapsulation efficiency and a novel technique to assess lipid-protein interaction, Pharmaceutical Research. 29 (2012) 1919–1931.

[48] E. Ravazzolo, S. Salmaso, F. Mastrotto, S. Bersani, E. Gallon, P. Caliceti, pH-responsive lipid core micelles for tumour targeting, European Journal of Pharmaceutics and Biopharmaceutics. 83 (2013) 346–357.

[49] V.A. Sethuraman, K. Na, Y.H. Bae, pH-responsive sulfonamide/PEI system for tumor specific gene delivery: an in vitro study, Biomacromolecules. 7 (2006) 64–70.

[50] T. Chanmee, P. Ontong, K. Konno, N. Itano, Tumor-Associated Macrophages as major players in the tumor microenvironment, Cancers. 6 (2014) 1670–1690.

[51] S. Bersani, M. Vila-Caballer, C. Brazzale, M. Barattin, S. Salmaso, pH-sensitive stearoyl-PEG-poly(methacryloyl sulfadimethoxine) decorated liposomes for the delivery of gemcitabine to cancer cells, European Journal of Pharmaceutics and Biopharmaceutics. 88 (2014) 670–682.

[52] Y. Nie, L. Ji, H. Ding, L. Xie, L. Li, B. He, Y. Wu, Z. Gu, Cholesterol derivatives based charged liposomes for doxorubicin delivery: preparation, in vitro and in vivo characterization, Theranostics. 2 (2012) 1092–1103.

[53] F. Atyabi, A. Farkhondehfai, F. Esmaeili, R. Dinarvand, Preparation of pegylated nano-liposomal formulation containing SN-38: in vitro characterization and in vivo biodistribution in mice, Acta Pharmaceutica. 59 (2009).

[54] M. Rovira-Bru, D.H. Thompson, I. Szleifer, Size and structure of spontaneously forming liposomes in lipid/PEG-lipid mixtures, Biophysical Journal. 83 (2002) 2419–2439.

[55] S. Salmaso, P. Caliceti, Stealth properties to improve therapeutic efficacy of drug nanocarriers, Journal of Drug Delivery. 2013 (2013) 374252–19.

[56] E. Ravazzolo, S. Salmaso, F. Mastrotto, S. Bersani, E. Gallon, P. Caliceti, pH-responsive lipid core micelles for tumour targeting, European Journal of Pharmaceutics and Biopharmaceutics. 83 (2013) 346–357.

[57] A.J. Reisinger, S.H. Tannehill-Gregg, C.R. Waites, M.A. Dominick, B.E. Schilling, T.A. Jackson, Dietary ammonium chloride for the acidification of mouse urine, J. Am. Assoc. Lab. Anim. Sci. 48 (2009) 144–146.

[58] R.A. Fenton, C.-L. Chou, G.S. Stewart, C.P. Smith, M.A. Knepper, Urinary concentrating defect in mice with selective deletion of phloretin-sensitive urea transporters in the renal collecting duct, Proc. Natl. Acad. Sci. U.S.a. 101 (2004) 7469–7474.

[59] J.D. Cook, K.A. Strauss, Y.H. Caplan, C.P. Lodico, D.M. Bush, Urine pH: the effects of time and temperature after collection, J Anal Toxicol. 31 (2007) 486–496.

[60] B. Roy, P. Guha, R. Bhattarai, P. Nahak, G. Karmakar, P. Chettri, A.K. Panda, Influence of lipid composition, pH, and temperature on physicochemical properties of liposomes with curcumin as model drug, J Oleo Sci. 65 (2016) 399–411.

[61] J. Meyer, L. Whitcomb, D. Collins, Efficient encapsulation of proteins within liposomes for slow release in vivo, Biochemical and Biophysical Research Communications. 199 (1994) 433–438.

[62] W. Chanput, J.J. Mes, H.F.J. Savelkoul, H.J. Wichers, Characterization of polarized THP-1 macrophages and polarizing ability of LPS and food compounds, Food Funct. 4 (2013) 266–276.

[63] F. Chen, G. Zhang, Y. Cao, M.J. Hessner, W.A. See, MB49 murine urothelial carcinoma: molecular and phenotypic comparison to human cell lines as a model of the direct tumor response to Bacillus Calmette-Guerin, The Journal of

Urology. 182 (2009) 2932–2937.

[64] G. Zhao, L.B. Rodriguez, Molecular targeting of liposomal nanoparticles to tumor microenvironment, International Journal of Nanomedicine. Volume 8 (2012) 61–71.

[65] C. Kelly, C. Jefferies, S.-A. Cryan, Targeted liposomal drug delivery to monocytes and macrophages, Journal of Drug Delivery. 2011 (2011) 727241–11.

[66] N.-B. Hao, M.-H. Lü, Y.-H. Fan, Y.-L. Cao, Z.-R. Zhang, S.-M. Yang, Macrophages in tumor microenvironments and the progression of tumors, Clinical and Developmental Immunology. 2012 (2012) 1–11.

[67] M.M. D'Elios, A. Amedei, A. Cappon, G. Del Prete, M. de Bernard, The neutrophil-activating protein of Helicobacter pylori (HP-NAP) as an immune modulating agent, FEMS Immunology & Medical Microbiology. 50 (2007) 157–164.

[68] H.J. Kang, J.-M. Ha, H.S. Kim, H. Lee, K. Kurokawa, B.L. Lee, The role of phagocytosis in IL-8 production by human monocytes in response to lipoproteins on Staphylococcus aureus, Biochemical and Biophysical Research Communications. 406 (2011) 449–453.

[69] H. Zhu, Y. Shi, W. Tang, G. Shi, H. Wan, Inhaled corticosteroid influence toll like receptor 2 expression in induced sputum from patients with COPD, Translational Respiratory Medicine. 1 (2013) 7.

[70] G.P. Andrews, T.P. Laverty, D.S. Jones, Mucoadhesive polymeric platforms for controlled drug delivery, European Journal of Pharmaceutics and Biopharmaceutics. 71 (2009) 505–518.

Graphical abstract